IEEE Access
Multidisciplinary | Rapid Review | Open Access Journal

Received November 2, 2017, accepted November 22, 2017, date of publication December 7, 2017,
date of current version February 14, 2018.

Digital Object Identifier 10.1109/ACCESS.2017.2780889

A Comparative Experimental Study of Robust Sliding Mode Control Strategies for Underactuated Systems

SAMI UD DIN[1], (Member, IEEE), QUDRAT KHAN[2], FAZAL UR REHMAN[1], AND RINI AKMELIAWANTI[3], (Senior Member, IEEE)

[1]Department of Electrical Engineering, Capital University of Science and Technology, Islamabad 44000, Pakistan
[2]Center for Advance Studies in Telecommunications, COMSATS Institute of Information Technology, Islamabad 44000, Pakistan
[3]Department of Mechatronics Engineering, International Islamic University, Kuala Lumpur 50728, Malaysia

(Corresponding author: Sami Ud Din (samiuddin@ieee.org)

This work was supported by the Higher Education Commission, Government of Pakistan.

ABSTRACT This paper presents a comprehensive comparative study for the tracking control of a class of underactuated nonlinear uncertain systems. A given nonlinear model of the underactuated system is, at first stage, transformed into an input output form and the driving applied control input of the transformed system is then designed via four sliding mode control strategies, i.e., conventional first order sliding mode control, second order sliding mode, fast terminal sliding mode, and integral sliding mode. At second stage, a ball and beam system is considered and the aforementioned four control design strategies are experimentally implemented. A comprehensive comparative study of the simulation and experimental results is then conducted which take into account the tracking performance, i.e., settling time, overshoots, robustness enhancement, chattering reduction, sliding mode convergences, and control efforts.

INDEX TERMS Electromechanical system, sliding mode control, Lyapunov method, robust control, nonlinear systems.

I. INTRODUCTION

The under-actuated systems, which have fewer number of control input than their degrees of freedom, attracted a great number of researchers [1]. The under-actuation makes their control distinct from other nonlinear systems such as fully-actuated systems. This feature can be introduced in system design specially, for cost minimization and weight reduction (like in space applications). This feature may also be caused by the system dynamics and actuator malfunctioning [2]. In addition, one may introduce this under-actuation deliberately for creating low-order nonlinear systems for the aim of getting an insight in the control of high order underactuated systems e.g., a ball and beam systems [3], inverted pendulum systems [4], translational oscillator with rotational actuator (TORA) [5]. This class finds very interesting applications in humanoids, aerospace systems and underwater vehicles, mobile and locomotive systems. In order to operate such kind of systems autonomously, very sophisticated control techniques are required.

In the context of control design, broad range of control techniques are available for fully actuated systems. However, for underactuated systems the problem definition and control design vary from system to system. The control design techniques employed so far are adaptive control [6], feedback linearization [7], passivity based control [8] and optimal control [9], etc. However, these strategies may not be employed for a large class of underactuated systems where linearization becomes difficult via smooth feedback [10]. In addition, Brockett necessary condition is also not satisfied by the majority of underactuated systems [11]. In the context of feedback linearization, the researchers have established the collocated and non-collocated partial feedback linearization approaches for these systems [7], [12]. However, such techniques are inapplicable to flat underactuated systems e.g., inertia-wheel pendulum (IWP) and vertical take-off and landing (VTOL) aircraft [12]. Passivity based methodology is also suggested for underactuated systems [13]. However, passivity based approach can be applied to systems having degrees of freedom (DOF) less than two [12]. This is a main drawback of the passitivity based approach. To overcome the limitations of passivity approach, back-steeping based technique is proposed in [14]. This methodology is effective

for global stabilization of underactuated systems with low DOF [15]. However, computational complexities increase with the increase in the DOF. In addition, the applications of back-stepping technique to practical systems are unrealistic, due to increase in complexity level as DOF increases [12]. In the recent developments, fuzzy and neural network based control strategies (see for instance, [16]–[18]) are also used for the set-point regulation [19] and tracking control problems [20] of underactuated systems. These strategies are usually synthesized with other control design methodologies to develop new adaptive control and robust control techniques.

In practice, robustness is ever demanding in the employment of control strategies. In this regards, sliding mode control (SMC) based design approaches were focused in recent years for controlling underactuated systems (see for instance., [3], [21], [22]). However, the SMC suffers from a dangerous chattering phenomena, and in real applications, this may result in the wear tear of the actuators. Therefore, higher order sliding mode control (HOSMC) was proposed for this class to suppress the amplitude of the chattering [1], [23]. It is evident that as the order of sliding mode increases, the precision, robustness as well as accuracy decreases. Apart from the robustness, in practice, the precision is very demanding which can be achieved via finite time stabilization. It is claimed that finite time stabilization can be achieved by the use of fast terminal sliding mode control (FTSMC) in close loop [4]. In is worthy to mention that SMC, HOSM and TSMC cannot guarantee the invariance property in the necessary reaching phase. Therefore, to mitigate this threat, an integral sliding mode (ISM) based strategy was proposed in [10], which established sliding mode without reaching phase.

In this work, a comprehensive comparative study for the tracking control of a class of underactuated nonlinear uncertain systems is presented. A given nonlinear model of the underactuated system is, at first stage, transformed into an input output form and the driving applied control input of the transformed system is then designed via four sliding mode control strategies i.e., conventional first order sliding mode control (FOSMC), second order sliding mode (SOSMC), fast terminal sliding mode (FTSMC), and integral sliding mode (ISM). At second stage, a ball and beam system is considered and the aforementioned four control design strategies are experimentally implemented. A comprehensive comparative study of the simulation and experimental results is then conducted which takes into account the tracking performance i.e., settling time, overshoots, robustness enhancement, chattering reduction, sliding mode convergences and control efforts. It is preferable that the contributions in this work is three fold i.e., the system transformation into canonical form by defining a suitable output, the simulation as well as practical implementation of the four control strategies and the comparative analysis of the said techniques. The rest of the papers presented in the following manner.

Section II contributes the general presentation and problem formulation for the specified class. The control law designs of the SMC, SOSMC, ISMC and FTSMC are presented in Section III of the paper. Section IV presents the development of the control laws, simulation, and practical results of the ball and beam system. Section V concludes the comparative study followed by recent supporting references.

II. PROBLEM FORMULATION

The equations of motion for the class of underactuated nonlinear systems are generally expressed as follows [10]:

$$M(q)\ddot{q} + C(q,\dot{q})\dot{q} + G(q) + F(\dot{q}) = B(\rho + \delta(q,\dot{q},t)) \quad (1)$$

where $q, \dot{q} \in R^n$ represents the position and velocity states vectors which make a configuration space of $2n$ variable (or states), $M(q) \in R^{n\times n}$ is the inertia matrix, $C(q,\dot{q}) \in R^{n\times n}$ is the matrix describes the centrifugal and coriolis forces, $G(q) \in R^{n\times 1}$ is gravitational force vector and $F(\dot{q}) \in R^{n\times n}$ represents fractional torque. B is the control input channel, and $\rho \in R^m$ such that $m < n$ represents the applied control input. The nonlinear term $(M^{-1}(q)B)$ takes into account the uncertainties in the control input channel. Since we consider the system to be controllable, therefore, before proceeding to the problem formulation we assume that$(M^{-1}(q)B)$ is full rank and the origin serves as an equilibrium point.

Now by following the strategy of [24], the nonlinear system (1), can be represented via the following cascade form:

$$\begin{cases} \dot{x}_1 = x_2 + d_1 \\ \dot{x}_2 = f_1(x_1,x_2,x_3,x_4) + d_2 \\ \dot{x}_3 = x_4 \\ \dot{x}_4 = f_2(x_1,x_2,x_3,x_4) + b(x_1,x_2,x_3,x_4)\rho + d_3 \end{cases} \quad (2)$$

where x_1, x_2, x_3, x_4 are the available states of the system, d_1, d_2 and d_3 are bounded disturbances, $f_1(x_1,x_2,x_3,x_4)$ and $f_2(x_1,x_2,x_3,x_4)$ are nonlinear smooth functions. The nonlinear smooth function $b(x_1,x_2,x_3,x_4)$ represents the control input channel and ρ is the applied controlled input. Note that system (2) is an alternate form of system (1) such that the first two equations in (2) represent the indirectly controllable subsystem with state variables x_1 and x_2, and the last two equations in (2) represent the directly control- influenced system with state variables x_3 and x_4. Regarding the cascaded form (2) the following assumptions are made.

Assumption 1: It is assumed that $b(x_1,x_2,x_3,x_4)$ is nonzero everywhere in the available space. This assumption confirms the controllability of the given nonlinear system.

Assumption 2: Assume that

$$f_1(0,0,0,0) = 0 \quad (3)$$

Equation (3) confirms that the origin is an equilibrium point in close loop.

Assumption 3: $\frac{\partial f_1}{\partial x_3}$ is invertible or $\frac{\partial f_1}{\partial x_4}$ is invertible which, in other words, confirms the controllability of the given nonlinear system.

Assumption 4: $f_1(0,0,x_3,x_4) = 0$ is an asymptotically stable manifold, i.e. x_3 and x_4 approaches zero.

Now, we make the following remark.

Remark 1: Since every control methodology can be easily employed to controllable canonical forms, therefore, we aim to transform the newly established form (2) to a controllable canonical form. In this way, one may eliminate the required condition on the disturbances d_1, d_2 and d_3 [22]. In addition, one can easily employ the so far available techniques. Such formats are applicable for nonlinear systems like TORA, quad rotor [25] and inverted pendulum [4].

It is worthy to note that Assumptions 3 and 4 are non-necessary conditions. These are used when one needs to furnish the closed loop system with a sliding mode controller, for details see [22]. Now, by following the procedure defined by [10], the system shown in (2) can be transformed into the following input-output form:

$$\begin{cases} \dot{\xi}_1 = \xi_2 \\ \dot{\xi}_2 = \xi_3 \\ \vdots \\ \dot{\xi}_n = \varphi(\xi, \rho) + \gamma(\xi)\{\rho + \Delta G_m(\xi, \rho, t)\} \end{cases} \tag{4}$$

In (4), $\xi = [\xi_1, \xi_2, \cdots, \xi_n]^T$ represents the state vector and $\Delta G_m(\xi, \rho, t)$ indicates the matched uncertainties. The symbol ρ is the applied control input. Note that the nonlinear dynamics of an inverted pendulum, double inverted pendulum, ball and beam system, and flexible joints manipulator of link 1 can be easily replaced in the above equivalent input output form. Before the design it is suitable to assume that:

Assumption 5: The uncertainty is assumed to be bounded i.e.,

$$|\Delta G_m(\xi, \rho, t) \leq \Gamma| \tag{5}$$

In realistic sense this assumption means that the uncertainty have a tolerable magnitude. Now, the problem in hand is the design of a controller for system (4). Having controlled (4) will imply a clear solution to the control problem of system (2). The core control problem of system (4) is to steer the real state to zero i.e., a regulation problem is considered. This task is fulfilled via a family of control strategies i.e., FOSMC, SOSMC, ISMC and FTSMC while considering the system subject to matched disturbances. At this stage we are now ready to pursue for its control design via the aforementioned family of sliding mode controllers.

III. CONTROL LAW DESIGN

In this section the control design for the system (4) is presented via a family of sliding mode control strategies. Here we proceed by designing the control law via FOSMC, SOSMC, ISMC and FTSMC.

A. SLIDING MODE CONTROL

The sliding mode control (see for more detail [26]) is always considered as an effective and efficient approach in control systems because of its invariance in sliding mode i.e., it results in robustness against uncertainties in sliding mode. The design of SMC usually supports systems which have relative degree one with respect to the sliding manifold. The control law is always composed of two components i.e., an equivalent control component and a discontinuous control component. Mathematically, it can be expressed as follows:

$$\rho = \rho_{eq} + \rho_{sw} \tag{6}$$

In order to design a control law, at first step a switching manifold of the following form is considered.

$$\sigma(\xi) = \sum_{i=1}^{n} c_i \xi_i \tag{7}$$

Computing the time derivative of (7) along (4) one may have

$$\dot{\sigma}(\xi) = c_1\xi_2 + \ldots + c_i\xi_{i+1} + \varphi(\xi, \rho) + \gamma(\xi)\rho \tag{8}$$

Now by posing $\sigma(\xi) = 0$, one get

$$\rho_{eq} = -\frac{1}{\gamma(\xi)}\left(\varphi(\xi, \rho) + \sum_{i=1}^{n} c_i\xi_{i+1}\right) \tag{9}$$

To design the discontinuous control component, a Lyapunov of the following form is defined.

$$V(\xi) = \frac{1}{2}\sigma^2 \tag{10}$$

Calculating the time derivative of this function along (4) and then substituting (9), one may get

$$V(\xi) = \sigma(\xi)\left(\gamma(\xi)\Delta G_m(\xi, \rho, t) + \rho_{sw}\right) \tag{11}$$

Now by choosing the expression of the discontinuous term as follows:

$$\rho_{sw} = -Ksign(\sigma) \tag{12}$$

$$\dot{V}(\xi) \leq -|\sigma|\left[-K + |\gamma(\xi)\Delta G_m(\xi, \rho, t)|\right] \tag{13}$$

By using the bound of uncertainties (5), one has

$$\dot{V}(\xi) \leq -|\sigma|\left[-K + |\gamma(\xi)\Delta G_m(\xi, \rho, t)|\right] \tag{14}$$

This can also be expressed as

$$\dot{V}(\xi) \leq -|\sigma|\,\iota \leq 0 \tag{15}$$

provided that

$$K \geq [K_M\Gamma + \iota] \tag{16}$$

where ι and Γ are positive constants and K_M is the maximum absolute value of $\gamma(\xi)$. The inequality in (15) confirms that $\sigma(\xi)$ approaches zero in a finite time t_s [27]. Consequently, the states of the system (4) will be steered to the origin via the control law defined in (6) with detailed expressions in (9) and (12). In SMC, the controller suffers from high frequency vibration in sliding mode phase. In order to reduce this dangerous vibration, in the next subsection, the same problem is handled with second order sliding modes.

Remark II: The most prominent advantage of the first order SMC is the order reduction in sliding mode. This order reduction results in insensitivity to disturbances and model uncertainties. However, to keep the sliding mode the control input has to switch with infinite frequency along a sliding constraint. This switching causes a severe damage in the system components. This characteristic is no more advantageous in the real word and even degrades the sliding modes fascination.

B. SECOND-ORDER SLIDING MODE CONTROL

Since the drawback of the conventional SMC is chattering effect [28], which degrades the system performance and may lead towards system instability. Therefore, the removal of chattering was focused by a wide number of researchers. In literature, the saturation function is used instead of the discontinuous function [29]. However, in this case the robustness as well as accuracy is partially lost. The other main stream approach was the use of an observer-based approach which results in less magnitude of the uncertain term [30]. Consequently, the chattering was suppressed. In the context of chattering removal, the most famous approach was the HOSM control technique [31]. In this approach the sliding mode occurs along the intersection of the sliding variable and its derivative of order r. In this case, the sliding set is defined to be $\sigma = \ddot{\sigma} = \dddot{\sigma} = \ldots = \sigma^{(r-1)} = 0$. The structure of the controller is designed in such a way that it confirms finite time enforcement of sliding mode along the defined sliding set in the presence of the disturbances/uncertainties which in turn results in increased accuracy of the sliding modes and output convergence. Moreover, the increase in the order of sliding mode results in reduced chattering. However, the robustness decreases. In the literature the most famous and appealing relative degree one higher order sliding mode controller is the super twisting (STW) which has considerable robustness with acceptable chattering reduction. We now intend to design super-twisting controller for this class of nonlinear systems.

1) SUPER-TWISTING SLIDING MODE CONTROL

In this design the sliding set consists of the intersection of hyper planes $\sigma(\xi) = 0$ and $\dot{\sigma}(\xi) = 0$ i.e., the sliding mode occurs on the following set

$$\sigma(\xi) = \dot{\sigma}(\xi) = 0 \tag{17}$$

Since STW deals with relative degree one case [31], therefore, the sliding variable (7) is quite suitable for this design strategy. Now, by taking the time derivative of (7), along (4) one get

$$\dot{\sigma}(\xi) = \sum_{i=1}^{n-1} c_i \xi_{i+1} \tag{18}$$

or

$$\dot{\sigma}(\xi) = c_1\xi_2 + \ldots + c_i\xi_{i+1} + \varphi(\xi, \rho) + \gamma(\xi)\rho \tag{19}$$

This can also be realized as

$$\dot{\sigma}\ (\xi) = \psi_1\ (\xi) + \gamma\ (\xi)\ \rho \tag{20}$$

where

$$\psi_1\ (\xi) = c_1\xi_2 + \ldots + c_i\xi_{i+1} + \varphi(\xi, \rho) \tag{21}$$

By following [1], the control law can be expressed as:

$$\rho = \frac{\rho_1 - \psi_1\ (\xi)}{\gamma\ (\xi)} \tag{22}$$

where ρ is chosen according to the strategy of [32] as follows:

$$\begin{cases} \rho_1 = -k_1 sign\ (\sigma)\ |\sigma_i|^{\frac{1}{2}} - k_2\sigma + \omega \\ \dot{\omega} = -k_3 sign\ (\sigma) - k_4\sigma \end{cases} \tag{23}$$

In expression (23), k_i; $i = 1, 2, 3, 4$ are positive gains. If one chose k_i according to [33]. Then the finite time enforcement of sliding mode against $\sigma_i = \dot{\sigma}_i = 0$ can be ensured. The chattering attenuation is a considerable advantage of the STW and it remains insensitive to bounded perturbations, but these perturbations cannot increase faster than a linear function of time or it can be said that they do not need to be bounded [34]. For the stability and detailed proof one may read [32]. The sliding mode control strategy remains very sensitive to disturbances in the reaching phase which may decrease the applicability of this technique. Therefore, a reaching phase free sliding mode control was proposed which enhances the robustness from the very beginning and considerably reduces chattering (see for details [26]). In the subsequent study, an integral sliding mode for the system (4) is designed.

Remark III: Since the conventional SMC causes wear tear on the system components, therefore, one of the main challenge which was solved via the second order sliding mode was the chattering attenuation. This technique on one hand keep the main characteristics of first order SMC i.e., order reduction and on the other hand, suppresses chattering. In addition, this technique makes easy the practical implementation. However, one must be clear that the robustness in this technique decreases, as the order of sliding mode increase.

C. INTEGRAL SLIDING MODE CONTROL

This technique retains the main features of the sliding mode with enhanced robustness against matched disturbances with attenuated chattering across the switching manifold. Generally, the control law for ISM can be expressed as follows:

$$\rho = \rho_0 + \rho_1 \tag{24}$$

where the first component on the right hand side of the above equation governs the system dynamics during sliding modes whereas the matched disturbances have been compensated by the second component. The sliding surface of ISM is defined as:

$$\sigma\ (\xi) = \sum_{i=1}^{n} c_i\xi_i + z \tag{25}$$

Now, by adapting the strategy proposed in [10], the control structure can be chosen as follows:

$$\rho = -K_0^T\xi - \frac{1}{\gamma\ (\xi)}(\varphi\ (\xi, \rho) + (\gamma\ (\xi) - 1)\ \rho_0 + Ksign\sigma \tag{26}$$

where

$$\dot{z} = -\left(\sum_{i=1}^{n-1} c_i\xi_{i+1} + \rho_0\right), \tag{27}$$

$$\rho_0 = -K_0^T\xi \tag{28}$$

and

$$\rho = -\frac{1}{\gamma(\xi)}\left(\varphi(\xi,\rho) + (\gamma(\xi)-1)\rho_0 + Ksign\sigma\right) \quad (29)$$

The initial condition of (27) are chosen such that the manifold remains at zero at the initial time $t = 0$ i.e., $z(0) = -\sigma_0(\xi(0))$ should be justified. For more details, one may read [10]. This control law (26) establishes sliding mode from the very start of the process and confirms the regulation of the states of the system (4) to zero under the action of (28).

Remark IV: This design technique offers a number of advantages. The most promising one is the establishment of sliding mode from the very start of the processes i.e., no reaching phase happens. Hence the system becomes more robust from the initial time instant. In addition, the unwanted chattering phenomena can be suppressed up to considerable order. However, no order reduction happens which consequently makes the system sensitive to parametric variations. This sensitivity to parameter can be reduced by designing a continuous control component of the controlled input more cleverly.

D. FAST TERMINAL SLIDING MODE CONTROL

It is evident that the asymptotic convergence in the absence of a strong force may not deliver fast convergence. The conventional terminal sliding mode control, on the other hand, may not confirm fast convergence when the system states have initial conditions quite away from the equilibrium. However, the fast terminal sliding is capable to combine the advantages of both SMC and TSM and can make the convergence to the equilibrium faster. This job can be done via changing the definition of the switching manifold. Therefore, in this section, the fast terminal sliding mode for the class of underactuated system (4) is designed. Another main aim of the use of this strategy is to acquire high precision tracking with suppressed chattering. The sliding surface of fast terminal sliding mode controller is designed as follows [35]:

$$\sigma(S(\xi)) = \dot{S}(\xi) + \alpha_1 S(\xi) + \beta_1 (S(\xi))^{\frac{p_1}{q_1}}, \quad (30)$$

where $S(\xi)$ can be defined as:

$$S(\xi) = \sum_{i=1}^{n-1} c_i \xi_i \quad (31)$$

The gains α_1 and β_1 in (30) are positive constants, p_1 and q_1 are positive odd integers such that p_1 should be greater than q_1. The time derivative of (30) along (4) takes the form:

$$\dot{\sigma}(S(\xi)) = \begin{pmatrix} \sum_{i=1}^{n-1} c_i \xi_{i+1} + \varphi(\xi,\rho) + \gamma(\xi)\rho \\ +\alpha_1 \dot{S}(\xi) + \frac{p_1}{q_1}\beta_1 (S(\xi))^{\frac{p_1}{q_1}-1} \dot{S}(\xi) \end{pmatrix} \quad (32)$$

By following the design strategies [4] and [35], the final control law can be expressed as follows:

$$\rho = -(\gamma(\xi))^{-1} \begin{pmatrix} \sum_{i=1}^{n-1} c_i \xi_{i+1} + \varphi(\xi,\rho) + \alpha_1 \dot{S}(\xi) \\ + \frac{p_1}{q_1}\beta_1 (S(\xi))^{\frac{p_1}{q_1}-1} \dot{S}(\xi) \\ + Ksign(\sigma) \end{pmatrix} \quad (33)$$

In order to prove the stability of FTSMC for system (4) the readers may follow strategies of [4] and [35]. This design strategy confirms fast convergence of the system's states to the equilibrium with high precision and suppress chattering phenomena. Now, at this stage, the aforesaid design techniques are required to be tested on an experimental setup. Therefore, in the forthcoming section, all the controllers are implemented on an actual underactuated ball and beam system.

Remark V: The FTSMC use a sliding manifold which not only results in the finite time enforcement of sliding mode, but also confirms the systems states convergence in finite time. This finite time convergence result in high precision which makes this system more appealing in practical systems. Like conventional SMC its preserve robustness in sliding mode with considerably reduced chattering. The main disadvantages of this technique is the singularity occurrence as the order of the system increases. In addition, which treating different systems which deal hydrodynamics force result in an unknown sign of the Lyapunov derivative. Hence, stability becomes questionable.

IV. BALL AND BEAM EXAMPLE

This section is dedicated to present an illustrative example of the class of underactuated nonlinear systems which are influenced via the control law design in the previous section. A comprehensive comparative simulation and experimental study is the core of the following study.

A. SYSTEM DESCRIPTION AND CONTROL DESIGN

The proposed system is a sound candidate for the considered class. This system is known for its ill-defined relative degree with non-linear nature and its wide range of applications like, balancing liquids or fuel in linear moving vehicles as well as in vertical take-off objects and balancing of passenger cabin. The schematic diagram of ball on a beam system is shown in Fig. 1 and its typical parameters are reported in Table 1. In general, this setup consists of a metallic ball which rolls on a metallic beam of a finite length. In this equipment, one end of beam is fixed and other is connected to an electric servo motor to move the beam up and down. This system is designed for feedback strategies which work on the measured position of ball on the beam and the angle traced by the servo motor. In other words, the feedback takes into account the ball position and the motor angle.

The motion governing equations of the ball and beam system are taken from [10]:

$$\begin{cases} \left(mr^2 + T_1\right)\ddot{\beta} + (2mr\dot{r} + T_2)\dot{\beta} \\ \quad + \left(mgr + \frac{L}{2}Mg\right)\cos\beta = \rho, \\ T_4\ddot{r} - r(\ddot{\beta}^2) + gsin\beta = 0 \end{cases} \quad (34)$$

where $\theta(t)$ angle subtended to make stable the ball, the lever angle is represented by $\beta(t)$, $r(t)$ is the position of the ball on the beam and $v_{in}(t)$ is the input voltage of the motor whereas the controlled input appears mathematically via the

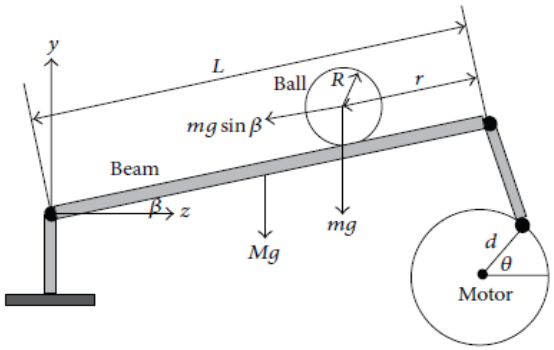

FIGURE 1. Schematic diagram of the ball on a beam system.

TABLE 1. Parameters and values used in equation.

Symbol	Quantity	Units	Values
g	Gravitational acceleration	m/s^2	9.81
m	Mass of ball	kg	0.04
M	Mass of beam	kg	0.15
L	Length of beam	m	0.4
R_m	Resistance of armature of the motor	Ω	9
J_m	Moment of inertia of motor	Nm/(rad/s^2)	7.35×(10)$^{-4}$
C_m	Torque constant of motor	Nm/A	0.0075
C_g	Gear ratio	--	4.28
d	Radius of arm connected to servo motor	m	0.04
J_l	Moment of inertia of beam	kgm^2	0.001
C_b	Back *emf* constant value	V/(rad/s)	0.5625

expression $\rho(t) = C_3 v_{in}(t)$ in the dynamic model. The derived parameters used in (34) are represented by T_1, T_2, T_3 and T_4 with the following mathematical relations [3]

$$\begin{cases} T_1 = \dfrac{R_m \times J_m \times L}{C_m \times C_b \times d} + J_1 \\ T_2 = \dfrac{L}{d}\left(\dfrac{C_m \times C_b}{R_m} + C_b + \dfrac{R_m \times J_m}{C_m \times C_g}\right) \\ T_3 = 1 + \dfrac{C_m}{R_m} \\ T_4 = \dfrac{7}{5} \end{cases} \tag{35}$$

The state space model is constructed by assuming $x_1 = r$ (represents the position of the ball on a beam), $x_2 = \dot{r}$ (rate of change of position), β is assumed to be as x_3 (beam angle) and $x_4 = \dot{\beta}$ (rate of change of motor angle). Following these definitions, one may get

$$\begin{cases} \dot{x}_1 = x_2 \\ \dot{x}_2 = \dfrac{1}{T_4}(-g sin(x_3)) \\ \dot{x}_3 = x_4 \\ \dot{x}_4 = \dfrac{1}{mx_1^2 + T_1}\left(\rho - (2mx_1x_2 + T_2)\, x_4 - \left(\begin{matrix} mgx_1 \\ +\dfrac{L}{2}Mg \end{matrix}\right) cosx_3\right) \end{cases} \tag{36}$$

Now, the output of interest is $y = x_1$, which represents the position of the ball. This representation is similar to that of (4). Now, the system is ready for the controller design.

B. CONTROLLER DESIGN

Following the procedure outlined in Section III, we proceed as follows

$$y = x_1, \tag{37}$$

$$\dot{y} = x_2, \tag{38}$$

$$\ddot{y} = -\frac{g}{T_4} sin(x_3), \tag{39}$$

$$y^{(3)} = -\frac{g}{T_4} x_4 cos(x_3), \tag{40}$$

$$\begin{aligned} y^{(4)} = {} & \frac{1}{T_4\left(mx_1^2 + T_1\right)}[-\rho cosx_3 + (2mx_1x_2 + T_2)\, x_4 cosx_3 \\ & + \left(mgx_1 + \frac{L}{2}Mg\right) cos^2 x_3 + x_4^2\left(mx_1^2 + T_1\right) \sin x_3], \end{aligned} \tag{41}$$

$$y^{(4)} = f_s + h_s \rho \tag{42}$$

$$f_s = \frac{g}{T_4}\left[\begin{matrix} \dfrac{(2mx_1x_2 + T_2)x_4 + (mgx_1 + L/2Mg)cosx_3}{(mx_1^2 + T_1)} \\ \times cosx_3 + x_4^2 sinx_3 \end{matrix}\right]$$

$$h_s = -\frac{g}{(T_4(mx_1^2 + T_1))} \times cosx_3$$

Now, writing in the controllable canonical form, defines in (4), for $n = 4$, one gets

$$\begin{cases} \dot{\xi}_1 = \xi_2, \\ \dot{\xi}_2 = \xi_3, \\ \vdots \\ \dot{\xi}_4 = \varphi(\xi, \rho) + \gamma(\xi)\rho + \gamma(\xi)\Delta G_m(\xi, \rho, t) \end{cases} \tag{43}$$

where $y^{(i-1)} = \xi_i$

$$\varphi(\xi) = f_s = \frac{g}{T_4}\left[\begin{matrix} \dfrac{(2mx_1x_2 + T_2)x_4 + (mgx_1 + L/2Mg)cosx_3}{(mx_1^2 + T_1)} \\ \times cosx_3 + x_4^2 sinx_3 \end{matrix}\right] \tag{44}$$

$$\gamma(\xi) = h_s = -\frac{g}{(T_4(mx_1^2 + T_1))} \times cosx_3 \tag{45}$$

and $\gamma(\xi)\Delta G_m(\xi, \rho, t)$ represents the matched uncertainties.

1) SLIDING MODE CONTROL (SMC)

Here we discuss conventional SMC on the ball and beam system. Sliding manifold defined in (7), is considered for $n = 4$ in following equation:

$$\sigma(\xi) = c_1\xi_1 + c_2\xi_2 + c_3\xi_3 + \xi_4 \tag{46}$$

Computing the time derivative of (46) along (43) one may have

$$\dot{\sigma}(\xi) = c_1\xi_1 + c_2\xi_2 + c_3\xi_3 + \dot{\xi}_4 \tag{47}$$

Further, after substituting (37-42), we got

$$\dot{\sigma} = c_1 x_2 + \frac{c_2}{T_4}(-gsin(x_3)) - \frac{c_3 g}{T_4} x_4 cos(x_3) + f_s + h_s \rho \tag{48}$$

Following the procedure laid in Section III-A, the complete control structure becomes:

$$\rho = \frac{1}{h_s}\left[-c_1 x_2 - \frac{c_2}{T_4}(-gsin(x_3)) + \frac{c_3 g}{T_4} x_4 cos(x_3) - f_s\right] - Ksign(\sigma) \tag{49}$$

where ρ_{eq} and ρ_{sw} are written as (50) and (51), respectively.

$$\rho_{eq} = \frac{1}{h_s}\left[-c_1 x_2 - \frac{c_2}{T_4}(-gsin(x_3)) + \frac{c_3 g}{T_4} x_4 cos(x_3) - f_s\right] \tag{50}$$

$$\rho_{sw} = -Ksign(\sigma) \tag{51}$$

As the control objective is to perform the reference tracking here, therefore, the sliding manifold and the controller will appear as follows:

$$\sigma(\xi) = c_1(\xi_1 - r_d) + \sum_{i=2}^{4} c_i \xi_i \tag{52}$$

$$\rho = \frac{1}{h_s}\left[-c_1 x_2 - \frac{c_2}{T_4}(-gsin(x_3)) + \frac{c_3 g}{T_4} x_4 cos(x_3) - f_s\right] - Ksign(\sigma) \tag{53}$$

where r_d is the desired reference with $\dot{r}_d, \ddot{r}_d, \dddot{r}_d$ are bounded.

2) SECOND ORDER SLIDING MODE CONTROL (SOSMC)

By following the procedure defined in Section III-B, the sliding manifold σ for super twisting sliding mode control remains the same as defined in (46) for $n = 4$. Since reference tracking is objective, therefore, the sliding manifold appears as follows:

$$\sigma(\xi) = c_1(\xi_1 - r_d) + c_2\xi_2 + c_3\xi_3 + \xi_4 \tag{54}$$

and the final structure of the control input is calculated as follows:

$$\rho = -k_1 sign(\sigma)|\sigma|^{\frac{1}{2}} - k_2\sigma - \int(-k_3 sign(\sigma) - k_4\sigma) \tag{55}$$

3) INTEGRAL SLIDING MODE CONTROL (ISMC)

In case of ISMC, the integral manifold defined in (25) can be defined as follows for the ball and beam system.

$$\sigma(\xi) = c_1(\xi_1 - r_d) + \sum_{i=2}^{4} c_i\xi_i + z \tag{56}$$

The final expression of the controller takes the form:

$$\rho = -k_1(\xi_1 - r_d) - k_2\xi_2 - k_3\xi_3 - k_4\xi_4 + \frac{1}{\gamma(\xi)}(-\varphi(\xi,\tau) - (\gamma(\xi) - 1)\rho_0 - Ksign(\sigma)) \tag{57}$$

TABLE 2. Parametric values used in the tracking for FOSMC, SOSMC(STW), ISMC and FTSMC.

FOSMC								
Constants	C_1	C_2	C_3	K_1	K_2	K_3	K_4	K
In Simulation	80	48	24	-	-	-	-	50
In Practical Implementation	9	4	1	-	-	-	-	1
SOSMC(STW)								
Constants	C_1	C_2	C_3	K_1	K_2	K_3	K_4	K
In Simulation	80	48	14	37	0	2	0	25
In Practical Implementation	5	29	5	0.5	0	0.1	0	5
ISMC								
Constants	C_1	C_2	C_3	K_1	K_2	K_3	K_4	K
In Simulation	1.2	1.2	0.11	402.98	250.18	60	4.1	5
In Practical Implementation	8	5	1	3	15	3	1	5
FTSMC								
Constants	C_1	C_2	C_3	α_1	β_1	p_1	q_1	K
In Simulation	100	70	10	2	0.11	1	9	12
In Practical Implementation	18	10	0.09	0.45	0.1	3	9	1

The dynamics of the integral term were calculated to be as follows

$$\dot{z} = c_1 x_2 + \frac{c_2 g}{C_4} sinx_3 + \frac{c_3 g}{C_4} x_4 cosx_3 - \gamma(\xi)\rho_0 - \varphi(\xi) \tag{58}$$

Note that the higher derivatives $\dot{r}_d, \ddot{r}_d, \dddot{r}_d$ of the reference trajectory were assumed to bounded.

4) FAST TERMINAL SLIDING MODE CONTROL (FTSMC)

In case of FTSMC for the considered ball and beam system with $n = 4$ the fast terminal manifold will be defined as follows:

$$\sigma(S(\xi)) = \dot{S}(\xi) + \alpha_1 S(\xi) + \beta_1 (S(\xi))^{\frac{p_1}{q_1}},$$

where $S(\xi) = c_1(\xi_1 - r_d) + c_2\xi_2 + \xi_3$ and p_1 and q_1 are positive odd integers. The final mathematical structure of the applied controller was selected as follows:

$$\rho = (h_s)^{-1}\begin{pmatrix} -f_s - c_2\xi_4 - c_1\xi_3 - \alpha_1(c_1\xi_2 + c_2\xi_3 + \xi_4) \\ -\frac{p_1}{q_1}\beta_1(c_1(\xi_1 - r_d) + c_2\xi_2 + \xi_3(\xi))^{\frac{p_1}{q_1}-1} \\ (c_1(\xi_2) + c_2\xi_3 + \xi_4) - Ksign(\sigma) \end{pmatrix} \tag{59}$$

C. SIMULATION RESULTS

In this study, the ball and beam system defined in (34) is operated under the action of the control laws (49), (55), (57) and (59). The gains used in controller during simulation are reported in Table II. The computer simulation of the overall closed loop system is carried by considering the reference tracking to be a fixed point $r_d(t)$ and the initial condition of the system was set to be $x_1(0) = 0.4$, $x_2(0) = x_3(0) = x_4(0) = 0$. The reference trajectory was defined to be

$$r_d(t) = 22cm, \quad t > 0 \tag{60}$$

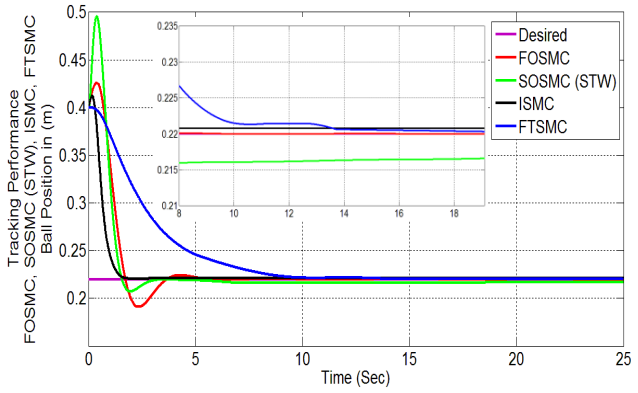

FIGURE 2. Output tracking performance of FOSMC, SOSMC(STW), ISMC and FTSMC, $r_d(t) = 22cm$.

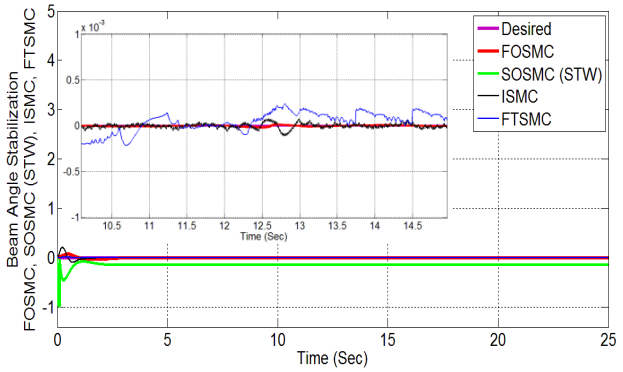

FIGURE 3. Beam angle stabilization profile of FOSMC, SOSMC (STW), ISMC and FTSMC, $r_d(t) = 22cm$.

The output tracking performance of all the four designed controllers is shown in Fig. 2. It can be clearly examined that the tracking performance of ISMC is very fast as compared to FOSMC and SOSMC. On the other hand, the performance of FTSMC is slower as compared to the remaining strategies. However, the precision of the FTSMC is very appealing. The zoomed version of reference tracking highlights the convergence precision of all the strategies.

The beam angle stabilization profile for FOSMC, SOSMC (STW), ISMC and FTSMC is displayed in Fig. 3. The separated profile of the beam angle stabilization can be seen in Fig. 4. The zoomed version of the angle stabilization shows the steady state error in case FTSMC as compared to the other stabilization strategies. In the beam angle stabilization, the FOSMC and ISMC are quite appealing. However, both techniques suffer from chattering which will be discussed in following study.

The sliding manifold comparison of all the techniques is shown in Fig 5 and 6 with their respective control inputs are displayed in Fig 7 and 8.

In case of manifold convergence, the SOSMC carries substantial marks as compared to its counter parts. However, in case of robustness enhancement and reaching phase elimination ISMC is far better than the others. In term of chattering

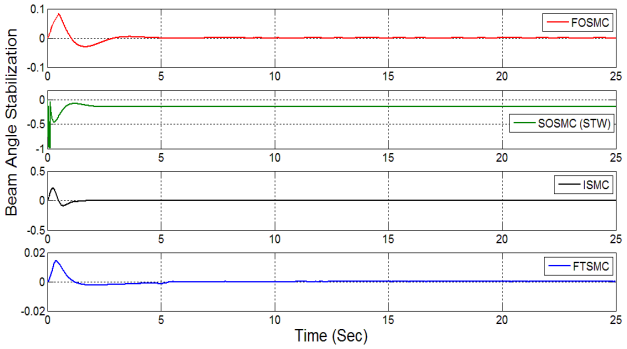

FIGURE 4. Separate beam angle stabilization profile of FOSMC, SOSMC(STW),ISMC and FTSMC.

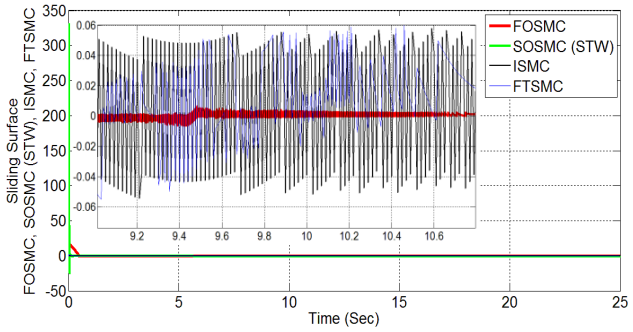

FIGURE 5. Sliding manifold convergence profile of FOSMC, SOSMC(STW), ISMC and FTSMC, $r_d(t) = 22cm$.

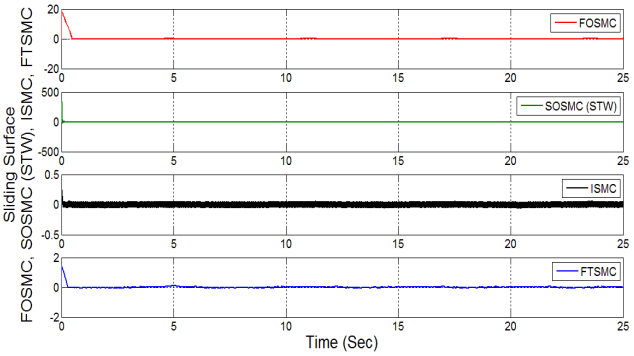

FIGURE 6. Separate sliding manifold convergence profile of FOSMC, SOSMC (STW), ISMC and FTSMC.

suppression, the FTSMC is better which makes it an appealing candidate in electromechanical systems.

However, the chattering may be reduced in case of ISMC by considering a strong reachability condition. Having chosen strong reachability condition, ISMC will outshine the remaining SMC variants.

Note that FOSMC in this case suffers from substantial magnitude of chattering which may cause the system failure. In case energy consumption, the ISMC and FTSMC utilize low energy as compared to FOSMC and SOSMC. Having analysed, in our views, the ISMC becomes an

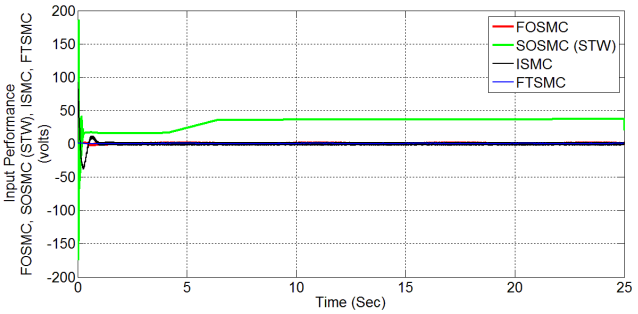

FIGURE 7. Control Input profile of FOSMC, SOSMC(STW), ISMC and FTSMC for reference tracking.

FIGURE 9. Experimental Setup of the Ball and Beam equipped via Googoltech GBB1004.

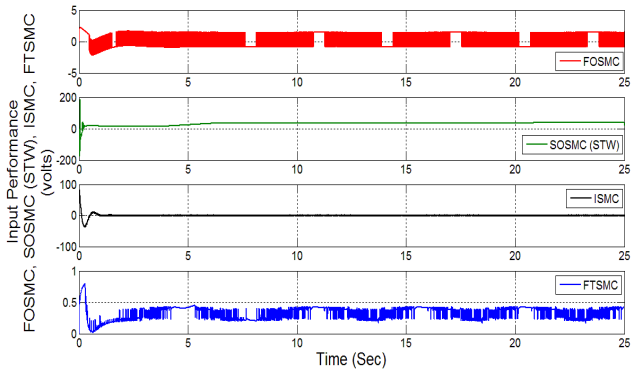

FIGURE 8. Separate control input profile of FOSMC, SOSMC(STW), ISMC and FTSMC.

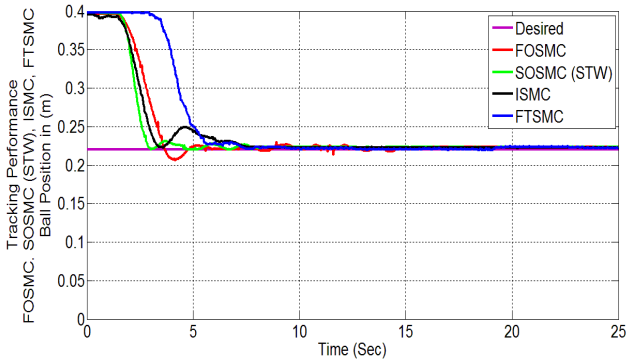

FIGURE 10. Output tracking performance of FOSMC, SOSMC(STW), ISMC and FTSMC, $r_d(t) = 22cm$.

appealing candidate to be employed to electromechanical systems.

D. EXPERIMENTAL RESULTS

In this study, the core objective is to keep the ball on a beam at the desired position $r_d(t)$. The control algorithms designed in the Section III, are implemented on the actual ball on a beam system. This system is manufactured by Googoltech GBB1004 with an intelligent IPM100 servo drive and electronic control box which supports the MATLAB 7.12/Simulink 7.7 environment. The other typical parameters includes the length of metallic beam with 40cm and a metallic ball of mass 40g. Fig 9 shows the experimental setup. The power module used in Googoltech requires 220V and 10A input. Note that the control accuracy of this equipment lies within the range of $\pm 1mm$.

During the practical implementation, the sampling time was chosen to be $2ms$. In order to make the implementation easy and simple, a time derivative block of the Simulink environment is used to provide the corresponding velocity measurements. The motor of the system is capable to rotate clockwise and anticlockwise to stabilize the ball. The physical components of the system have some limitations i.e., the steady state error must lie with the band of $\pm 0.001m$. In other words, this error will exist in case of any control strategy. The gains of the controller used during the implementation (experimentation) are reported in Table II.

The desired reference point on the beam was 22 cm. All the four techniques were implemented on the actual system and their tracking performances are displayed in Fig. 10 with zoomed results shown in Fig. 11. These results follow lies with in the vicinity of 0.22m which follow the physical limitation of the system. It is clear from Fig. 10 that the performance of the FTSMC and ISMC shows slower convergence to the reference point. However, the steady state error of these two techniques is quite smaller than the FOSMC and SOSMC. The precision of FTSMC carry comparatively high marks as compared to ISMC. It is noticeable that the ISMC result observe very little oscillations and shows a very stable behavior in the vicinity of the reference point. The results of SOSMC in this case is quite interesting and quite acceptable as compared to FTSMC and ISMC but it loses precision. The results of FOSMC are not acceptable because it exhibits oscillatory behavior along with low precision.

Remark VI: In the experimental study the translational position of the ball on a beam and the angular position of the driving motor are available. The respective velocities are calculated via the built in velocity estimator. However, one may use reduced order observer (see for instance [26] and [36]) for velocity estimation.

The comparative and separate beam angle stabilization profile for FOSMC, SOSMC (STW), ISMC and FTSMC are displayed in Figs. 12 and 13, respectively.

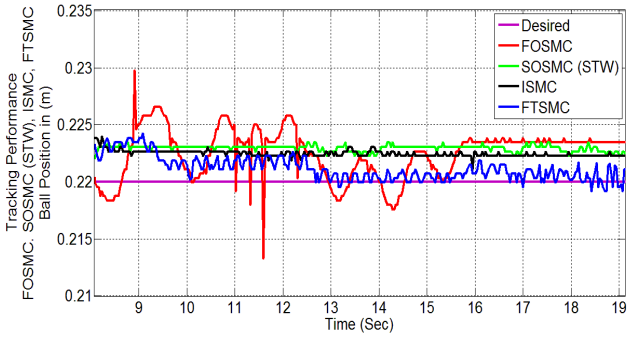

FIGURE 11. Zoom profile of output tracking performance of FOSMC, SOSMC(STW), ISMC and FTSMC.

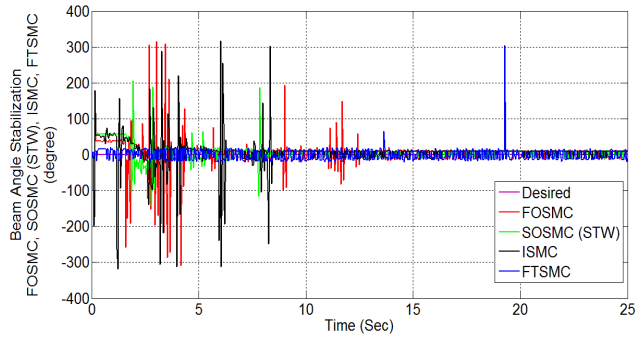

FIGURE 12. Beam angle stabilization profile of FOSMC, SOSMC(STW), ISMC and FTSMC, $r_d(t) = 22cm$.

It is worthy to notice that high chattering appear in the beam angle while implementing FOSMC. Comparatively small chattering appears in case of ISMC and SOSMC. However the beam angle of FTSMC exhibits with continuous chattering with sufficient small amplitude. Although it is tolerable for this system yet it is quite dangerous in practical systems when they are supposed to be operated for long time. In the author views, the ISMC and SOSMC are quite appealing in this case because once the angle is stabilized the system observes no chattering and in this case it may not be that harmful for the system health. We summarize this behavior as follows:

FOSMC:	have maximum (high amplitude) chattering,
SOSMC(STW):	have moderate chattering,
ISMC:	have (more than STW, less than FOSMC),
FTSM:	have minimal chattering but continuous.

The sliding manifold convergence comparison as well as separate profiles of all the techniques are shown in Figs. 14 and 15. The control efforts of these algorithms are also displayed in Figs. 16 and 17. It is clear that all the four controllers have stable sliding manifolds converge toward the origin. Fig. 15 experimentally verified the sliding mode enforcements. The manifold of the ISMC remains almost at zero which confirms the results achieved in the simulations (see Fig. 6). The manifold of the FTSMC observes

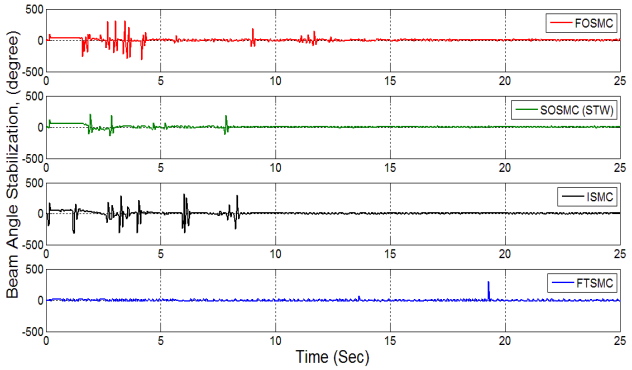

FIGURE 13. Separate beam angle stabilization profile of FOSMC, SOSMC(STW), ISMC and FTSMC.

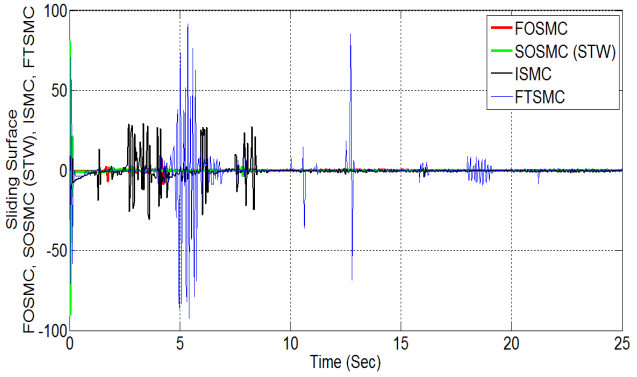

FIGURE 14. Sliding manifold convergence profile of FOSMC, SOSMC(STW), ISMC and FTSMC, $r_d(t) = 22cm$.

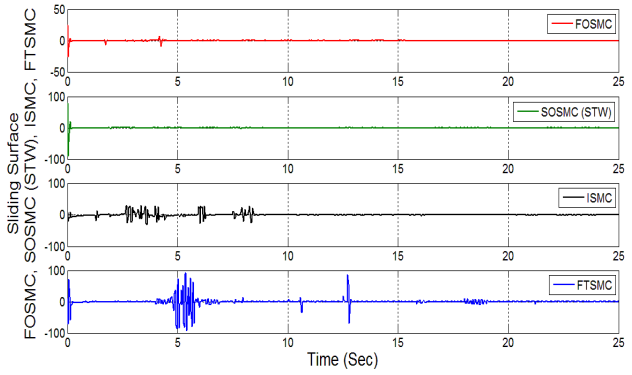

FIGURE 15. Separate sliding manifold convergence profile of FOSMC, SOSMC(STW), ISMC and FTSMC.

some heavy peaks which may threat the systems health. The SOSMC and FOSMC manifold convergence is somewhat interesting. On the other hand, the control efforts of FTSMC is quite higher even when the system is in sliding mode. This behavior reduces the applicability of FTSMC. While looking at FOSMC control efforts and SOSMC efforts, they fascinate the control designer to use these two strategies. However, the tracking behaviors of both these techniques disappoints

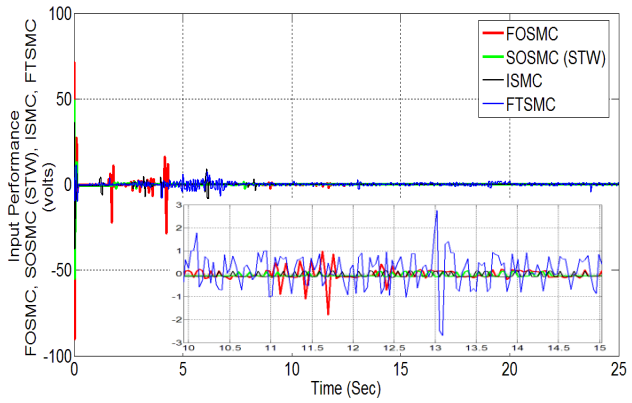

FIGURE 16. Control Input profile of FOSMC, SOSMC(STW), ISMC and FTSMC for reference tracking.

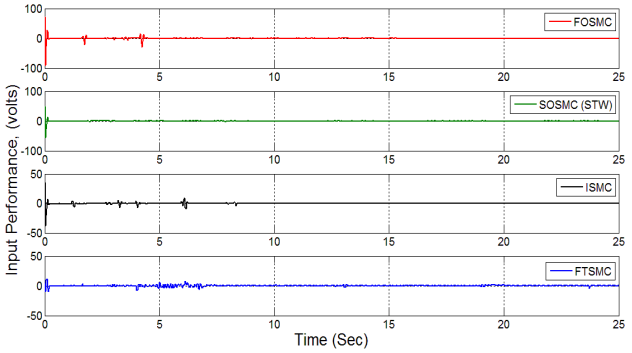

FIGURE 17. Separate control input profile of FOSMC, SOSMC(STW), ISMC and FTSMC.

TABLE 3. Comparison of energy criteria ($\times 10^4 J$).

FOSMC	SOSMC(STW)	ISMC	FTSMC
4.1072	3.2961	2.3461	2.5712

as compared to ISMC. In term of robustness ISMC remains more robust than the other the other three strategies because of the reaching phase elimination.

Further, on Googol tech GBB1004 platform, the utilized energy comparison among FOSMC, SOSMC(STW), ISMC and FTSMC is performed using the criteria presented in [1]:

$$J = \int_0^{15} u^2 dt \tag{61}$$

which is proportional to the energy delivered to the system. While comparing the energy utilization of these four algorithm, it comes out that ISMC utilizes minimum energy. The second minimum energy is utilized by the FTSMC. The third position is occupied by the SOSMC (see for details, Table III). The overall observations are summarized in the form of Table IV while examining different features in the experimental and simulation results.

Based on the attributes presented in Table IV, it can be claimed that ISMC proves itself to be an appealing control

TABLE 4. Comparitive analysis FOSMC, SOSMC(STW), ISMC and FTSMC.

Attributes	FOSMC	SOSMC (STW)	ISMC	FTSMC
Tracking Control	Slow (Not precise)	Slow (Not precise)	Very fast (Precise)	Slow (Highly precise)
Settling Time	Low	Low	Very low	High
Overshoot	High	Very high	Minimal	No overshoot
Chattering Analysis	Severe chattering	Low chattering	Minimal chattering	Moderate chattering
Sliding Surface Convergence	To origin, with chattering of medium magnitude amplitude	Remains at the origin with small magnitude oscillations in the very start	To origin, with moderate chattering amplitude	To origin, with considerable high chattering amplitude
Control Effort	Very high	High	Lowest	Low
Energy Utilization (in terms of Joule $\times 10^4 J$)	4.1075 (Maximum)	3.2961	2.3461 (Lowest)	2.5712
Computational Complexity	Low	High	High	High

protocol for the class of underactuated electro-mechanical systems.

V. CONCLUSION

A comprehensive comparative simulation and experimental study of the FOSMC, ISMC, SOSMC and FTSMC has been carried out in this work. The experimental step which was considered in this work was the ball and beam system. Before the design, the system was transformed to a controllable canonical form and then the control inputs were designed via the aforesaid strategies. The experimental and simulation study was carried out in the MATLAB environment. Having analysed, it was decided that ISMC carries marks in case of robustness and fast convergence with considerable suppression in chattering. However, in case of precision and chattering suppression the FTSMC can be preferred. The named FOSMC exhibits high frequency vibrations with considerable magnitude and with substantial steady state error whereas the SOSMC suffers from robustness issues in the reaching phase with considerable steady state error. The benefits of this study is to analyse the appealing attitude of FTSMC and ISMC in electromechanical systems.

REFERENCES

[1] S. Mahjoub, F. Mnif, and N. Derbel, "Second order sliding mode approaches for the class of under-actuated systems," *Int. J. Autom. Comput., Special Issue Adv. Nonlinear Dyn. Control*, vol. 12, no. 2, pp. 134–141, 2015.

[2] S. Mahjoub, F. Mnif, and N. Derbel, "Set point stabilization of a 2DOF underactuated manipulator," *J. Comput.*, vol. 6, no. 2, pp. 368–376, 2011.

[3] N. B. Almutairi and M. Zribi, "On the sliding mode control of ball on a beam system," *Nonlinear Dyn.*, vol. 59, nos. 1–2, pp. 221–238, 2010.

[4] Q. Khan, R. Akmeliawati, A. I. Bhatti, and M. A. Khan, "Robust stabilization of underactuated nonlinear systems: A fast terminal sliding mode approach," *ISA Trans.*, vol. 66, pp. 241–248, Jan. 2017.
[5] M. Jankovic, D. Fontanine, and P. V. Kokotovic, "TORA example: Cascade and passitivity-based control designs," *IEEE Trans. Control Syst. Technol.*, vol. 4, no. 3, pp. 292–297, Mar. 1996.
[6] Y. Fang, B. Ma, P. Wang, and X. Zhang, "A motion planning-based adaptive control method for an underactuated crane system," *IEEE Trans. Control Syst. Technol.*, vol. 20, no. 1, pp. 241–248, Jan. 2012.
[7] L. C. McNinch, H. Ashrafiuon, and K. R. Muske, "Sliding mode setpoint control of an underactuated surface vessel: Simulation and experiment," in *Proc. Amer. Control Conf.*, 2010, pp. 5212–5217.
[8] L. Freidovich, A. Shiriaev, F. Gordillo, F. Gómez-Estern, and J. Aracil, "Partial-energy-shaping control for orbital stabilization of high frequency oscillations of the furuta pendulum," *IEEE Trans. Control Syst. Technol.*, vol. 17, no. 4, pp. 853–858, Apr. 2009.
[9] E. C. Y. Yang, P. C. P. Chao, and C. K. Sung, "Optimal control of underactuated system for landing with desired postures," *IEEE Trans. Control Syst. Technol.*, vol. 19, no. 2, pp. 248–255, Feb. 2011.
[10] S. U. Din, Q. Khan, F. Rehman, and R. Akmeliawati, "Robust control of underactuated systems: Higher order integral sliding mode approach," *Math. Problems Eng.*, vol. 2016, Jan. 2016, Art. no. 5641478.
[11] R. W. Brockett, "Asymptotic stability and feedback stabilization," *Different Geometric Control Theory*, vol. 27, no. 1, pp. 181–191, 1983.
[12] Y. Liu and H. Yu, "A survey of underactuated mechanical systems," *Control Theory Appl., IET*, vol. 7, no. 7, pp. 921–935, May 2013.
[13] A. Shiriaev, A. Pogromsky, H. Ludvigsen, and O. Egeland, "On global properties of passivity-based control of an inverted pendulum," *Int. J. Robust Nonlinear Control*, vol. 10, no. 4, pp. 283–300, 2000.
[14] T. Madani and A. Benallegue, "Backstepping control for a quadrotor helicopter," in *Proc. IEEE/RSJ*, Beijing, China, Oct. 2006, pp. 3255–3260.
[15] K. D. Do, Z. P. Jiang, and J. Pan, "On global tracking control of a VTOL aircraft without velocity measurements," *IEEE Trans. Autom. Control*, vol. 48, no. 12, pp. 2212–2217, Dec. 2003.
[16] X. Zhao, H. Yang, W. Xia, and X. Wang, "Adaptive fuzzy hierarchical sliding-mode control for a class of MIMO nonlinear time-delay systems with input saturation," *IEEE Trans. Fuzzy Syst.*, vol. 25, no. 5, pp. 1062–1077, Oct. 2017.
[17] X. Zhao, P. Shi, X. Zheng, and J. Zhang, "Intelligent tracking control for a class of uncertain high-order nonlinear systems," *IEEE Trans. Neural Netw. Learn. Syst.*, vol. 27, no. 9, pp. 1976–1982, Sep. 2016.
[18] H. Wang, P. Shi, H. Li, and Q. Zhou, "Adaptive neural tracking control for a class of nonlinear systems with dynamic uncertainties," *IEEE Trans. Cybern.*, vol. 47, no. 10, pp. 3075–3087, Oct. 2017.
[19] C. W. Tao, J. S. Taur, T. W. Hsieh, and C. L. Tsai, "Design of a fuzzy controller with fuzzy swing-up and parallel distributed pole assignment schemes for an inverted pendulum and cart system," *IEEE Trans. Control Syst. Technol.*, vol. 16, no. 6, pp. 1277–1288, Nov. 2008.
[20] O. Begovich, E. N. Sanchez, and M. Maldonado, "Takagi-Sugeno fuzzy scheme for real-time trajectory tracking of an underactuated robot," *IEEE Trans. Control Syst. Technol.*, vol. 10, no. 1, pp. 14–20, Jan. 2002.
[21] H. Ashrafiuon, K. R. Muske, L. C. McNinch, and R. A. Soltan, "Sliding mode tracking control of surface vessels," *IEEE Trans. Ind. Electron.*, vol. 55, no. 11, pp. 4004–4012, Nov. 2008.
[22] R. Xu, and Ü. Özgüner, "Sliding mode control for a class of under-actuated systems," *Automatica*, vol. 44, no. 1, pp. 214–233, 2008.
[23] S. Riachy, Y. Orlov, T. Floquet, R. Santiesteban, and J. P. Richard, "Second order sliding mode control of underactuated mechanical systems I: Local stabilization with application to an inverted pendulum," *Int. J. Robust Nonlinear Control*, vol. 18, nos. 4–5, pp. 529–543, 2008.
[24] R. Olfati-Saber, "Normal forms for underactuated mechanical systems with symmetry," *IEEE Trans. Autom. Control*, vol. 47, no. 2, pp. 305–308, Feb. 2002.
[25] A. C. Satici, H. Poonawala, and M. W. Spong, "Robust optimal control of quadrotor UAVs," *IEEE Access*, vol. 1, pp. 79–93, 2013.
[26] V. Utkin, J. Guldner, and J. Shi, *Sliding Mode Control in Electromechanical Systems*. New York, NY, USA: Taylor & Francis, 1999.
[27] C. Edwards and S. K. Spurgeon, *Sliding Mode Control: Theory and Applications*. New York, NY, USA: Taylor & Francis, 1998.
[28] Y. B. Shtessel, J. A. Moreno, F. Plestan, L. M. Fridman, and A. S. Poznyak, "Super-twisting adaptive sliding mode control: A Lyapunov design," in *Proc. CDC*, 2010, pp. 5109–5113.
[29] H. Lee and V. I. Utkin, "Chattering suppression methods in sliding mode control systems," *Annu. Rev. Control*, vol. 31, no. 2, pp. 179–188, 2007.
[30] K. C. Veluvolu, Y. C. Soh, and W. Cao, "Robust observer with sliding mode estimation for nonlinear uncertain systems," *IET Control Theory Appl.*, vol. 1, no. 5, pp. 1533–1540, Sep. 2007.
[31] A. Levant, "Chattering analysis," *IEEE Trans. Autom. Control*, vol. 55, no. 6, pp. 1380–1389, Jun. 2010.
[32] I. Nagesh and C. Edwards, "A multivariable super-twisting sliding mode approach," *Automatica*, vol. 50, no. 3, pp. 984–988, 2014.
[33] J. A. Moreno and M. Osorio, "Strict Lyapunov functions for the super-twisting algorithm," *IEEE Trans. Autom. Control*, vol. 57, no. 4, pp. 1035–1040, Apr. 2012.
[34] L. Fridman, J. A. Moreno, B. Bandyopadhyay, S. Kamal, and A. Chalanga, "Continuous Nested Algorithms?: The Fifth Generation of Sliding Mode Controllers," *Recent Advances in Sliding Modes: From Control to Intelligent Mechatronics*, vol. 24, pp. 5–35, 2015.
[35] X. Yu and M. Zhihong, "Fast terminal sliding mode control design for nonlinear dynamical systems," *IEEE Trans. Circuit Syst.*, vol. 49, no. 2, pp. 261–264, Feb. 2002.
[36] S. Yin, H. Gao, J. Qiu, and O. Kaynak, "Descriptor reduced-order sliding mode observers design for switched systems with sensor and actuator faults," *Automatica*, vol. 76, pp. 282–292, Feb. 2017.

SAMI UD DIN (M'16) received the B.S. degree in electrical engineering from the Federal Urdu University of Arts, Science and Technology, Islamabad, Pakistan, in 2009, and the M.S. degree in electronics engineering with a specialization in control systems from Mohammad Ali Jinnah University, Islamabad, in 2012. He is currently pursuing the Ph.D. degree with the Capital University of Science and Technology, Islamabad.

His research interests include non-linear control, sliding mode control, and higher order sliding mode control with an emphasis toward underactuated systems.

QUDRAT KHAN received the B.Sc. degree in mathematics and computer science from the University of Peshawar in 2003, the M.Sc. and M.Phil. degrees in mathematics from Quaid-i-Azam University, Islamabad, in 2006 and 2008, respectively, and the Ph.D. degree in nonlinear control systems from Mohammad Ali Jinnah University, Islamabad, in 2012.

He was a Post-Doctoral Fellow with the Intelligent Mechatronics Systems Research Unit, International Islamic University, Malaysia, for one year. He is currently an Assistant Professor with the Center for Advanced Studies, Telecommunications, CIIT, Islamabad. He has authored over 30 research articles in refereed international journals and conference proceedings. His research interests include robust nonlinear control, observers/estimators design, and fault diagnosis of dynamic systems via sliding mode and its variants. He received the Postgraduate Scholarship during the Ph.D. from 2008 to 2011 and the IRSIP Scholarship during the Ph.D. (as a Visiting Research Scholar with the University of Pavia, Italy). He was selected for the Young Author Support Program, International Federation of Automatic Control, World Congress, Milan, Italy, in 2011.

FAZAL UR REHMAN received the M.Sc. and M.Phil. degrees in mathematics from Bahauddin Zakariya University, Multan, Pakistan, in 1986 and 1990, respectively, and the M.Eng. and Ph.D. degrees in control systems from the Department of Electrical Engineering, McGill University, Montreal, Canada, in 1993 and 1997, respectively.

From 1998 to 2001, he was an Assistant Professor with the Faculty of Electronic Engineering, Ghulam Ishaq Khan Institute of Engineering, Pakistan, where he was an Associate Professor from 2002 to 2006. Then he joined Mohammad Ali Jinnah University, Islamabad, Pakistan, as a Professor and HoD with the Department of Electronic Engineering in 2007. His research interests include nonlinear control systems, called nonholonomic control systems, multi rate digital signal processing, and optimal control.

RINI AKMELIAWANTI (M'04–SM'07) was born in Jakarta, Indonesia. She received the B.Eng. degree (Hons.) in electrical engineering from the Royal Melbourne Institute of Technology (RMIT) University, Australia, in 1997, and the Ph.D. degree in electrical and electronic engineering from the University of Melbourne, Australia, in 2002. She was a Lecturer with RMIT University from 2001 to 2004 and Monash University from 2004 to 2008. She is currently a Full Professor with the Department of Mechatronics Engineering, International Islamic University Malaysia. She has published over 150 international journal, book chapters, reviews, and conference papers. Her main research interests include nonlinear control systems theory and applications, intelligent systems, mechatronics, and signal and image processing. She was the Chair of the IEEE Instrumentation and Measurement Society–Malaysia Chapter from 2007 to 2009, where she was the Treasurer in 2010, and a Secretary of the IEEE Control Systems Society–Malaysia Chapter in 2010. She continuously serves the society as an Executive Committee Member. She is currently the Chair of the Intelligent Mechatronics System Research Unit, International Islamic University Malaysia. She is the Vice President of the Malaysian Society of Automatic Control Engineers. She is also a Co-Editor-in-Chief of the *International Journal of Robotics and Mechatronics*.